

Numerical and Parametric Study on RPV Lower Head Rupture Behavior

Ji-Hoon Kang^a, Tae-Hyun Kim^a and Yoon-Suk Chang^{a*}

^aDept. of Nuclear Engineering, Kyung Hee University, 1732 Deokyoungdae-ro, Yongin, Kyunggi, 446-701, Korea

*Corresponding author: yschang@khu.ac.kr

1. Introduction

As severe accidents of Nuclear Power Plants (NPPs) such as TMI, Chernobyl and Fukushima occur, the Reactor Pressure Vessel (RPV) lower head can be subject to high thermal loads due to corium [1]. Since the failure possibility of RPV lower head exists due to thermal load, phenomena of RPV under severe accident condition and strategies should be clearly understood and prepared in order to prevent the severe accidents. Strategies for coping with severe accidents, In-Vessel Retention through External Reactor Vessel Cooling (IVR-ERVC) [2, 3] and RPV depressurization were representatively adopted as a management strategy [4].

In this study, several parametric conditions of severe accident analysis were adopted to figure out the structural effects on RPV. The inner pressure of RPV was one of the most important factors which can affect the structural integrity. Damages due to high temperature and rupture of creep on the RPV lower head were direct risk of serious accidents, so it was necessary to evaluate the structural integrity in consideration of creep. However, most of the damage evaluation researches have been performed by considering elasto-plastic behavior. The steady-state does not take into account the actual operating pressure and temperature changes. Therefore, the influence of the pressure condition, creep behavior and treatment of steady or transient-state were analyzed. For the sake of damage evaluation, Larson-Miller Parameter (LMP) models were used to predict the creep damage factor and failure time.

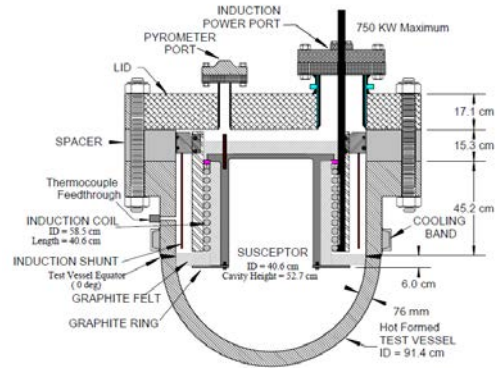
2. Numerical Analysis

2.1 Finite Element Model

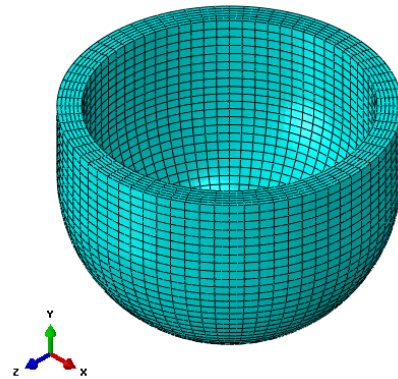
In early 2000s, Sandia National Laboratories (SNL) conducted the OECD / NEA Lower Head Failure project (OLHF) under the supervision of the Organization for Economic Cooperation and Development/Nuclear Energy Agency (OECD/NEA). The validity of the creep failure model was verified by comparing the analysis results with the experimental results. The lower head model considered in this study has 914.4mm in inner diameter, 1066.4mm in outer diameter, and 76mm in thickness as shown in Fig. 1(a) [4].

Fig. 1(b) represents the 3-D FE model for structural assessment. Commercial software ABAQUS ver. 6.14-5 used, DC3D20 (A 20-node quadratic heat transfer brick element) for heat transfer analysis and C3D20R (A 20-node quadratic brick and a reduced integration element)

for stress analysis were employed from the commercial program element library [5].



(a) OLHF test vessel with internal components [4]



(b) 3D model of finite element analysis

Fig. 1. RPV lower head

2.2 Analysis Condition

The thermal load condition required for the analysis used the internal surface temperature data of the OLHF experiment [4]. Total analysis time adopted as 11,200 s by taking into account the OLHF experiment condition. Ambient temperature and heat convection coefficient for heat transfer analysis were used for natural air cooling (Ambient temperature = 293K, $h = 10W/m^2-K$). Fig. 2 shows the pressure condition to the RPV lower head, and the upper surface of the lower head was fully fixed for the boundary condition. The material of the lower head was SA5331 and its material properties were referenced in the OLHF report [4].

For the parametric conditions that examined in this study, four cases are presented in Table I. Case 1 shows the transient-state analysis considering creep under high-pressure conditions. Case 2 shows a low-pressure analysis which different from Case 1 only in pressure

condition. Case 3 shows an elasto-plasticity analysis which does not consider creep. For the last, Case 4 shows different from steady-state condition but the others were same as Case 1.

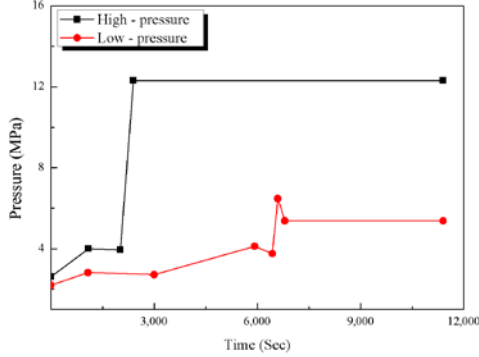


Fig. 2. Internal pressure of RPV lower head

Table I: Analysis cases

Case no.	Pressure	Condition	Time variable
1	High	Creep	Transient
2	Low	Creep	Transient
3	High	Elasto-plasticity	Transient
4	High	Creep	Steady-state

2.3 Creep and LMP Model

The creep constitutive equation based on the Bailey-Norton power series for general metal creep as shown in Eq. (1), and each constant applied with reference to the creep rupture test data [4].

$$\varepsilon = A\sigma^m t^n \quad (1)$$

where, σ is stress, A is the creep strain hardening coefficient, m and n are unitless constants, t is time that consistent with stress.

Damage evaluation carried out using the LMP model, which is mainly used. The general equation of LMP expressed by Eqs. (2) and (3).

$$LMP = T(C + \log_{10} t_{fail}) \quad (2)$$

$$\log_{10} \sigma = A - B(LMP) \quad (3)$$

where, T is the absolute temperature, t_{fail} time at failure occur, A , B and C is material constants. The material constants A , B and C were summarized in Table II using the LMP graph of pressure vessel material SA533B1 [4].

The failure time is calculated as the sum of the ratio of t_{fail} and incremental time which is calculated at each time increment. Eq. (4) predicts the actual rupture time using the cumulative damage fraction rule.

$$D(t + \Delta t) = D(t) + \frac{\Delta t}{t_{fail}} \quad (4)$$

where, D is the allowable creep damage factor generally set to 1.0 and Δt is time increment.

Table II: Constants of LMP

LMP	A	B	C
$T \geq 1050K$	4.1849	2.1165×10^{-4}	10.598
$T \leq 1050K$	5.9121	2.4506×10^{-4}	16.238

3. Analysis Results

3.1 Heat Transfer Analysis

For the central node is $\theta = 90^\circ$, the radiation cavity composed of an induction coil and a graphite susceptor located at about 70° of the internal surface of the lower head. As a result of the heat transfer analysis, the highest temperature occurred at 75° on the internal surface of the lower head of the transient-state. Temperature distribution at the end of the transient-state was shown in Fig. 3. Since high temperature occurred at $\theta = 75^\circ$, the points a , b and c along the thickness direction of RPV were selected to evaluate LMP damage evaluation.

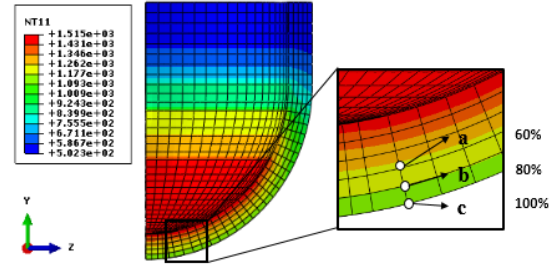


Fig. 3. Temperature distribution of RPV lower head

3.2 Structural Analysis

Fig. 4 shows the stress distribution at the central node of the lower head. When compared with the experiment, the stress variations were large during the transient process, but similarly decreased at the end of transients. Fig. 5 shows the stress analysis results at points a , b and c of the high temperature region. The lowest stress occurred in Case 2, which was performed under a low-pressure condition, and the largest stress generally occurred in Case 3, which was performed under an elasto-plastic analysis. The final stress values of Case 4 were shown in the graph as a single value. Steady-state indicates lower stress than transient-state analysis.

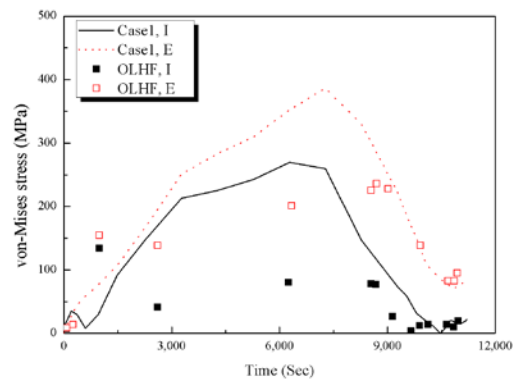


Fig. 4. Von-Mises stress at the central node

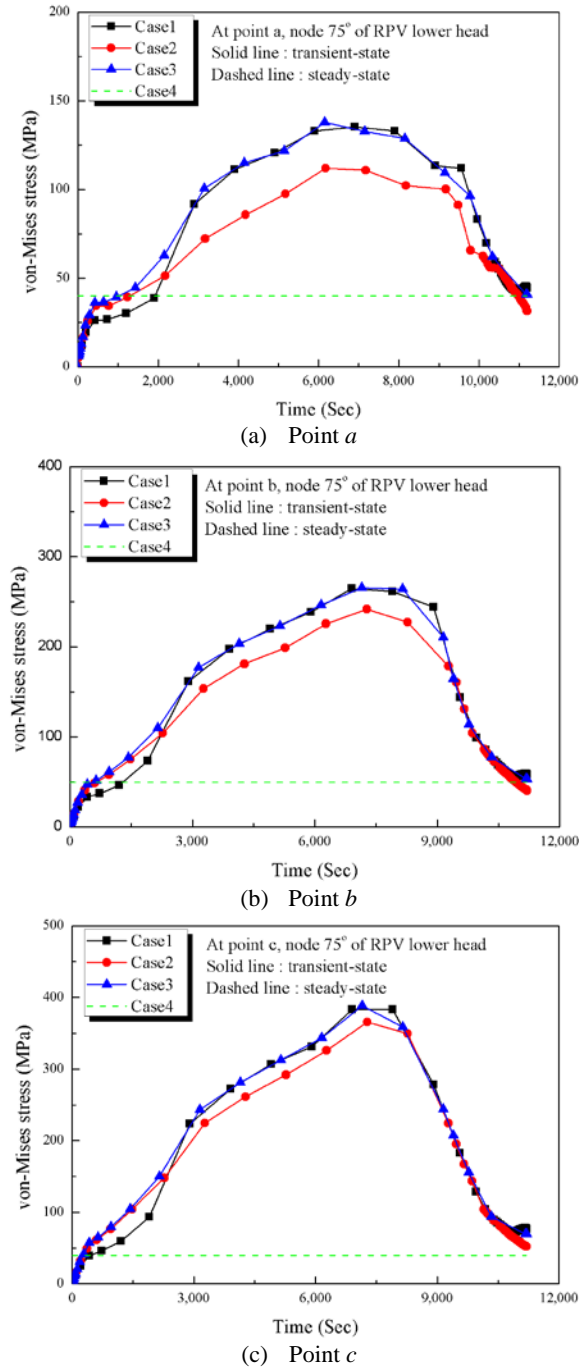


Fig. 5. Variation of von-Mises stresses at three points

3.3 Damage Evaluation

LMP damage evaluation were performed to calculate the rupture time for each case and the results were shown in Table III. Fig. 5 shows the variation of von-Mises stresses at three points. The rupture time of Case 2 was delayed than Case 3 because of the lower stress. The rupture time of Case 1 was slackened than Case 3 because of the lower stress at early phase of transient. If the operating conditions are maintained at steady-state temperature and stress, the lower head lasts for 0.2 s and rupture occurs.

Table III: LMP damage evaluation

Rupture time (sec)	Points along the thickness		
	<i>a</i>	<i>b</i>	<i>c</i>
Case 1	8,945	8,059	6,959
Case 2	9,105	8,322	7,304
Case 3	8,175	7,153	6,265
Case 4	0.239	0.267	0.222

4. Conclusions

In this paper, three parameters were determined and performed the finite element analysis. To predict the rupture time of RPV lower head, parametric study was conducted by LMP damage evaluation. Thereby, the following key findings were observed.

- (1) Under low – pressure conditions, low von-Mises stress occurs and rupture time is later. It can be confirmed that rupture time delayed under the condition of low – pressure in case of a severe accident.
- (2) The stress relaxation due to creep at the beginning of the transient period can be confirmed by comparing Case 1 and Case 3. Stress relaxation by creep causes slower rupture time than elasto–plastic analysis.
- (3) There was no significant difference between the steady–state and transient stress values but at the end of transient, steady–state indicates lower von-Mises stress. Since final stress value of the transient–state was larger, transient analysis was more reasonable than steady–state in terms of conservatism. But it was difficult to predict the rupture time accurately.
- (4) In the event of severe accident, the IVR-ERVC strategy can slow the damage of the external surface of RPV lower head but this study didn't consider the IVR-ERVC. As a result, natural convection cooling causes external surface rupture more quickly.

REFERENCES

- [1] T.H. Kim, S.H. Kim and Y.S. Chang, “Structural Assessment of Reactor Pressure Vessel under Multi-Layered Corium Formation Conditions”, Nuclear Engineering and Technology, Vol. 47, pp. 351-361, 2015.
- [2] R.J. Park, K.H. Kang and H.Y. Kim, Evaluation of corium behavior in the lower plenum of the reactor vessel during a severe accident, Nuclear Engineering and Design, Vol. 293, pp. 23-29, 2015.
- [3] T.I. Kim, H.M. Park and S.H. Chang, “CHF experiments using a 2-D curved test section with additives for IVR-ERVC strategy”, Nuclear Engineering and Design, Vol. 243, pp. 272-278, 2012.
- [4] OECD/NEA, “OECD Lower head failure project final report, Vol. 1 - integral experiments and material characterization”, 2002.
- [5] ABAQUS User's Manual, Ver.6-10.1, 2010, Dassault Systems.